# Structure−Activity Relationships of Carboline and Carbazole Derivatives as a Novel Class of ATP-Competitive Kinesin Spindle Protein Inhibitors

Tomoki Takeuchi,[†] Shinya Oishi,*,[†] Toshiaki Watanabe,[†] Hiroaki Ohno,[†] Jun-ichi Sawada,[‡] Kenji Matsuno,[‡] Akira Asai,[‡] Naoya Asada,[†] Kazuo Kitaura,[†] and Nobutaka Fujii*,[†]

[†]Graduate School of Pharmaceutical Sciences, Kyoto University, Sakyo-ku, Kyoto 606-8501, Japan
[‡]Graduate School of Pharmaceutical Sciences, University of Shizuoka, Suruga-ku, Shizuoka 422-8526, Japan

S Supporting Information

ABSTRACT: The kinesin spindle protein (KSP) is a mitotic kinesin involved in the establishment of a functional bipolar mitotic spindle during cell division. It is considered to be an attractive target for cancer chemotherapy with reduced side effects. Based on natural product scaffold-derived fused indole-based inhibitors and known biphenyl-type KSP inhibitors, various carboline and carbazole derivatives were synthesized and biologically evaluated. β-Carboline and lactam-fused carbazole derivatives exhibited remarkably potent KSP inhibitory activity and mitotic arrest in prometaphase with formation of an irregular monopolar spindle. The planar tri- and tetracyclic analogs inhibited KSP ATPase in an ATP-competitive manner just like biphenyl-type inhibitors.

ATP-competitive KSP inhibitors
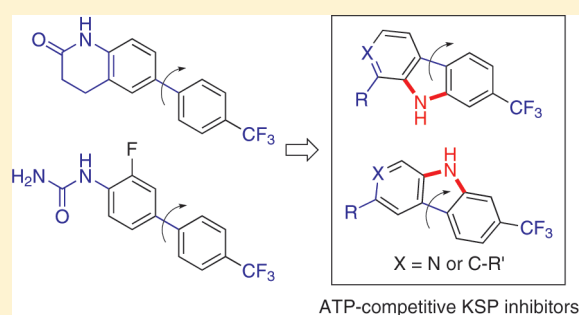
INTRODUCTION

Many studies have been carried out on the development of mitotic inhibitors. Most antimitotic agents (including taxanes and various vinca alkaloids) inhibit the function of the β-tubulin protein (a component of the microtubule), thereby showing anticancer activity.[1] However, the inhibition of microtubules leads to severe peripheral neuropathy because microtubules are also present in other nondividing cells (e.g., postmitotic neurons) and possess other critical physiological functions in cellular processes.[2] Acquired drug resistance is another obstacle after the long-term use of antimitotic agents. To overcome these limitations, novel anticancer agents with fewer adverse effects against other molecular targets are being developed.

The kinesin spindle protein (KSP; also known as Eg5) is a member of the kinesin-5 family. It plays an essential part in the formation and maintenance of the bipolar spindle. The KSP moves along antiparallel microtubules toward the plus end with energy from the hydrolysis of ATP, thereby separating centrosomes.[3] Inhibition of the KSP leads to mitotic arrest in prometaphase with irregular formation of the monopolar spindle and subsequent apoptotic cell death.[4] The KSP is abundantly expressed only in proliferating human tissues and not presented in postmitotic neurons in the human central nervous system, so the inhibitors might work as therapeutic agents with better selectivity for the treatment of malignant tumors.[5,6]

Recently, we reported that carbazoles 3a−c with a bulky alkyl group at the 2- or 3-position exhibited potent KSP inhibitory
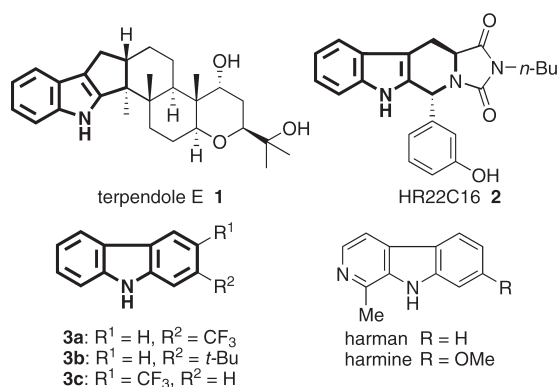

Figure 1. Structures of the reported KSP inhibitors **1** and **2** and the potent KSP inhibitors with a 2,3-fused indole substructure.

activity.[7] Based on the common substructure of the known KSP inhibitory terpendole E, **1**, and HR22C16, **2** (Figure 1),[8,9] the ring-fused indoles were identified to be minimal scaffolds for KSP inhibition. During the course of the study, it was also demonstrated that the cytotoxic activity of β-carboline alkaloids harman and harmine in part originated from KSP inhibitory activity.[7] Although these natural products and natural product-related
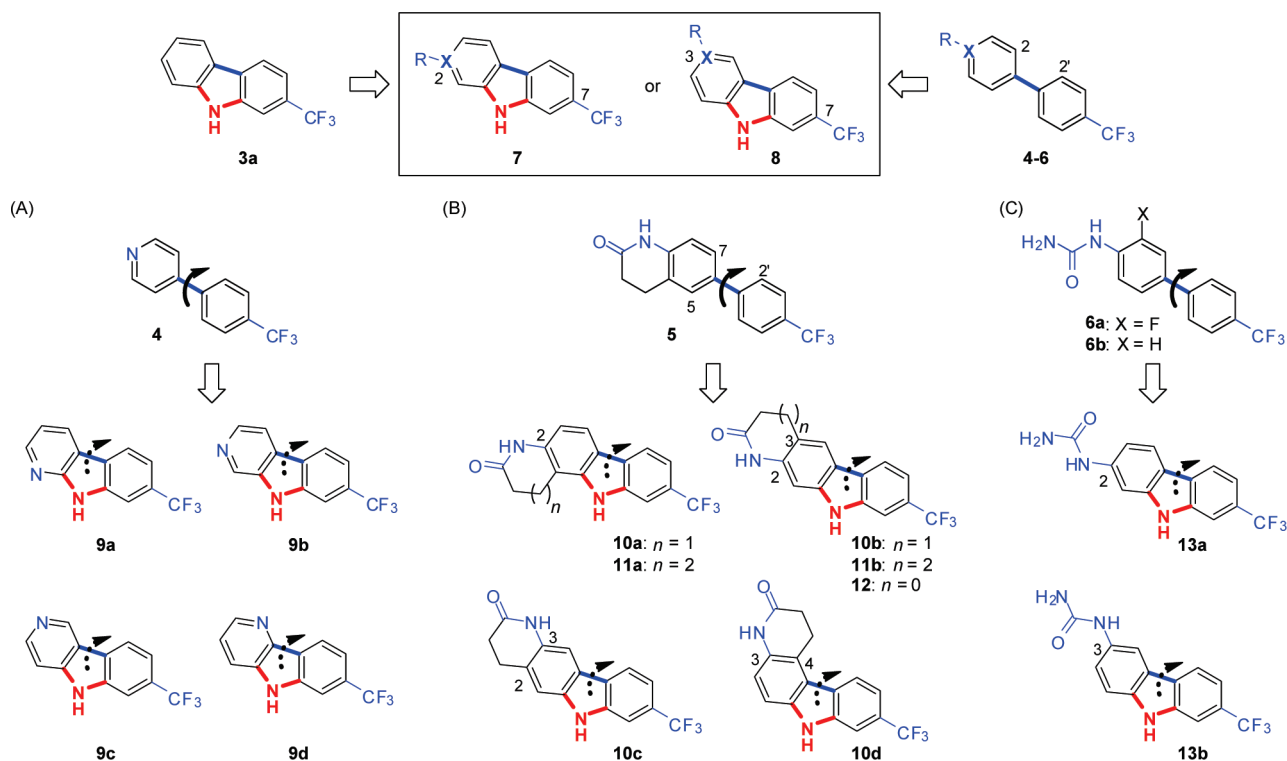
Figure 2. Design of novel KSP inhibitors 9−13 with fused indole scaffolds such as carboline (A) and carbazoles (B, C).

compounds include a complex structure with cyclic and acyclic accessory substituents, the identification of the core substructure facilitated further structure−activity relationship studies. Alternatively, KSP inhibitors with biaryl scaffolds such as 4−6 have been reported (Figure 2).[10] The biphenyls 5 and 6 bind to the interface of helices α4 and α6 (which is remote from the ATP binding site) to inhibit KSP activity in an ATP-competitive manner.[10b] We assumed that carbazole derivatives 3 with KSP inhibitory activity could be regarded as compounds with a nitrogen atom bridged between the 2- and 2′-carbons of biphenyl. Restriction of the rotatable bond could configure the coplanar conformation of biphenyl groups, as well as the appropriate orientations of the carbazole substituents, for binding to KSP with subsequent reduced entropy loss. Accordingly, reported herein is the design and synthesis of KSP inhibitors with planar carbazole and carboline scaffolds. Enzymatic analysis of the potent derivatives is also described to investigate the potential binding and functional modes of action.
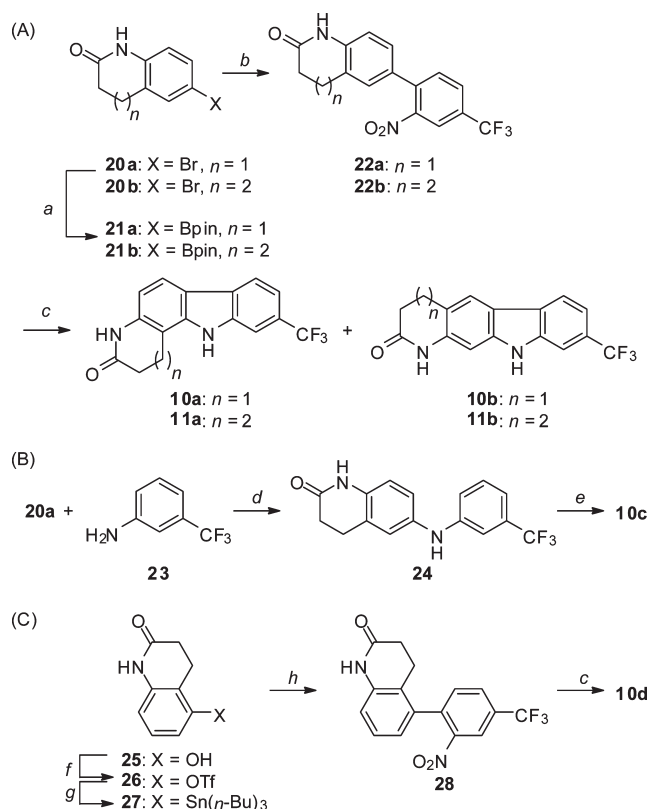
■ RESULTS AND DISCUSSION

Design of Potent KSP Inhibitors with a Ring-Fused Indole Scaffold. Two possible orientations of the accessory groups on the carbazole core were deliberated, when we focused on the rotatable biaryl C−C bond of the 1-aryl-4-(trifluoromethyl)-benzene scaffold in 4−6. Bidirectional orientations of 7 at the carbazole 2- and 7-positions were designed from ring-closing via one-nitrogen linkage between biphenyl 2- and 2′-positions. Reproduction of the outward-facing orientations of two accessory groups in the biaryl compounds 4−6 could provide the 3,7-disubstituted carbazoles 8.

Scheme 1. Synthesis of Carboline Derivatives[a]
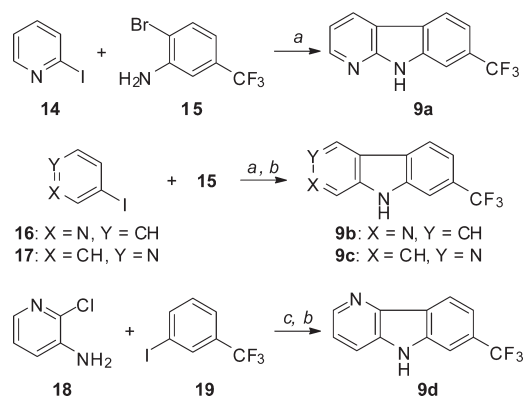
[a] Reagents and conditions: (a) Pd(OAc)$_2$, Xantphos, NaOt-Bu, toluene, reflux; (b) Pd(OAc)$_2$, PCy$_3$·HBF$_4$, K$_2$CO$_3$, t-BuCO$_2$H, DMA, 130 °C; (c) CuI, 1,10-phenanthroline, K$_2$CO$_3$, DMF, 110 °C.
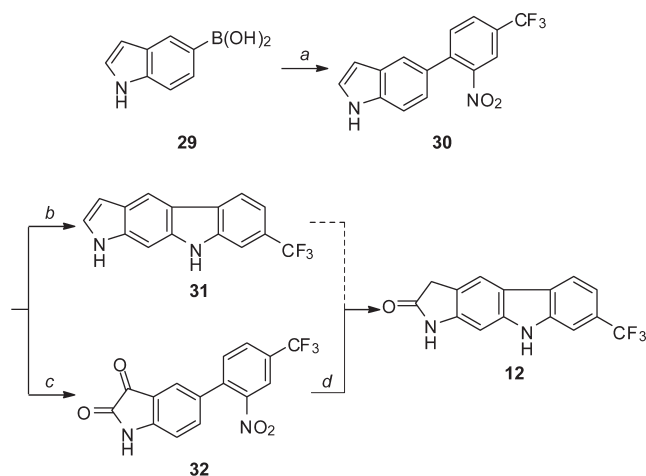
Carboline derivatives 9a−d with a 7-trifluoromethyl group were designed based on the 4-[4-(trifluoromethyl)phenyl]pyridine 4[11] with moderate KSP inhibitory activity (Figure 2A). β-Carboline 9b was designed to examine the restriction effect of the rotatable bond between benzene and the pyridine ring of compound 4, in which the 4-phenylpyridine framework was included in the 6−5−6 tricyclic structure of β-carboline. The arrangements of a pyridine nitrogen and a CF$_3$ group of γ-carboline 9c were presumably mimicked by the relative orientations of the pyridine nitrogen and the CF$_3$ group of 4. Additional α- and δ-carbolines 9a,d were the alternative regioisomers, which were incompatible with the conformations of 4-phenylpyridine derivative 4.

Scheme 2. Synthesis of Carbazole Derivatives with a Lactam-Fused Structure[a]

(A)

20a: X = Br, *n* = 1
20b: X = Br, *n* = 2

21a: X = Bpin, *n* = 1
21b: X = Bpin, *n* = 2

22a: *n* = 1
22b: *n* = 2

10a: *n* = 1
11a: *n* = 2

10b: *n* = 1
11b: *n* = 2

(B)

20a + **23** → **24** → **10c**

(C)

25: X = OH
26: X = OTf
27: X = Sn(*n*-Bu)₃

28 → **10d**

[a] Reagents and conditions: (a) (pinB)₂, PdCl₂(dppf), KOAc, DMSO, 80 °C; (b) 4-bromo-3-nitrobenzotrifluoride, PdCl₂(dppf), K₂CO₃, 1,4-dioxane, 90 °C; (c) PPh₃, *o*-DCB, 165 °C; (d) Pd₂(dba)₃·CHCl₃, DavePhos, NaO*t*-Bu, toluene, 100 °C; (e) Pd(OAc)₂, O₂, AcOH, 120 °C; (f) Tf₂O, pyridine, CH₂Cl₂, rt; (g) Pd(PPh₃)₄, LiCl, (Bu₃Sn)₂, 1,4-dioxane, 100 °C; (h) 4-bromo-3-nitrobenzotrifluoride, Pd₂(dba)₃·CH-Cl₃, P(*t*-Bu)₃·HBF₄, CsF, toluene, 110 °C.

Scheme 3. Synthesis of Carbazole Derivatives with a Five-Membered Lactam Ring or Pyrrole-Fused Structure[a]

29 → **30**

31

32

12

[a] Reagents and conditions: (a) 4-bromo-3-nitrobenzotrifluoride, Pd-(OAc)₂, XPhos, K₂CO₃, 1,4-dioxane, 60 °C; (b) 4-(dimethylamino)-triphenylphosphine, *o*-DCB, 160 °C; (c) PCC, 1,2-DCE, 80 °C; (d) 4-(dimethylamino)triphenylphosphine, *o*-DCB, 140 °C.

Dihydroquinolinone (GSK-1), **5**, is also a highly potent KSP inhibitor with a 4-trifluoromethylbiphenyl scaffold (Figure 2B), which presumably binds in a twisted conformation of the biphenyl part at the interface of the α4 and α6 helices of KSP.[10b] Mimicking the possible planar conformation of biphenyl-type **5**, we designed four lactam-fused carbazole derivatives **10a–d**. Carbazole **10a** or **10b** was designed by bridging via an NH group between dihydroquinolinone 5- or 7-positions and the 2′-position of **5**, respectively. In carbazoles **10c,d** with 2,3- and 3,4-fused lactams, the orientations of the trifluoromethyl and lactam anilide moieties in **5** were reproduced. To optimize the appropriate ring systems of **10a,b** for KSP inhibition, carbazoles **11a,b** and **12** with different ring-sized lactams were also evaluated. Carbazoles **13a,b** with a urea group at the 2- or 3-position were similarly investigated, which are the constrained analogs of a biphenyl **6a** (GSK-2) and nonfluorinated congener **6b** (Figure 2C).[12]

Synthesis of Carboline and Carbazole Derivatives for Potential KSP Inhibitors. A series of carboline derivatives **9a–d** were prepared by N-arylation using 2-, 3-, or 4-iodopyridine (**14**, **16**, **17**)/2-bromo-5-(trifluoromethyl)aniline (**15**) or 3-amino-2-chloropyridine (**18**)/substituted iodobenzene (**19**) and the subsequent palladium-catalyzed intramolecular C−H arylation of N-aryl-2-haloaniline derivatives (Scheme 1).[13]

For carbazoles **10a,b** with a six-membered lactam, aryl bromide **20a** was initially converted to pinacolboronate **21a**[14] by a palladium-catalyzed coupling reaction with bis(pinacolato)diboron.[15] The subsequent Suzuki−Miyaura cross-coupling of **21a** led to the 2-nitrobiphenyl derivative **22a** (Scheme 2A). The carbazoles **10a,b** were obtained by triphenylphosphine-mediated reductive cyclization of **22a**.[16] Carbazoles **11a,b** with a seven-membered lactam were also synthesized in a similar procedure. The other lactam-fused carbazole **10c** was obtained by palladium-catalyzed N-arylation of lactam **20a** and *m*-CF₃-substituted aniline **23** followed by oxidative biaryl coupling (Scheme 2B).[17] For the preparation of carbazole **10d**, phenol derivative **25** was initially converted to the corresponding trifluoromethanesulfonate **26** (Scheme 2C).[18] Next, organotin compound **27** was obtained by treatment of **26** with bis-(tributyltin) in the presence of a palladium catalyst and LiCl,[19] and subsequent Stille coupling with aryl bromide provided compound **28**.[20] The desired carbazole **10d** was prepared using identical conditions for the reductive cyclization.

The synthesis of carbazole **12** with a five-membered lactam was undertaken via indole derivative **30**, which was prepared using Suzuki−Miyaura coupling from commercially available boronic acid **29** (Scheme 3). Compound **30** was converted to carbazole **31** by phosphine-mediated reductive cyclization. However, separation of the byproduct triphenylphosphine oxide from the product **31** by repeated column chromatography failed. When 4-(dimethylamino)triphenylphosphine was used for the reducing reagent, the purification of carbazole **31** was readily achieved by a single round of column chromatography. Unfortunately, our efforts to obtain the desired carbazole **12** upon treatment with various oxidative reagents resulted only in the recovery or decomposition of **31**. As an alternative, an isatin derivative **32** was prepared by the oxidation of compound **30** using pyridinium chlorochromate (PCC).[21] Interestingly, when compound **32** was treated with 4-(dimethylamino)triphenyl-phosphine, the carbonyl group at the isatin 3-position was reduced

Scheme 4. Synthesis of Carbazole Derivatives with a Urea Group[a]
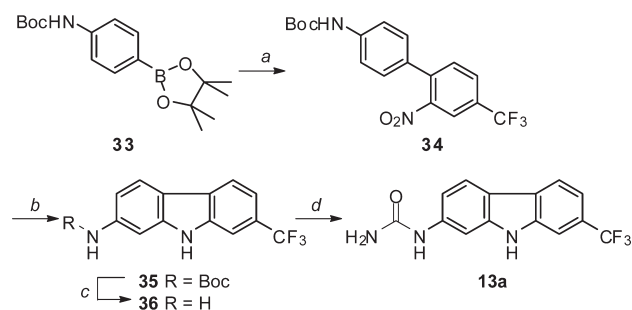
[a] Reagents and conditions: (a) 4-bromo-3-nitrobenzotrifluoride, PdCl$_2$-(dppf), K$_2$CO$_3$, 1,4-dioxane, 80 °C; (b) PPh$_3$, o-DCB, 165 °C; (c) 4 N HCl in 1,4-dioxane, rt; (d) KOCN, AcOH, H$_2$O, rt.
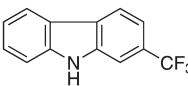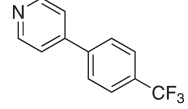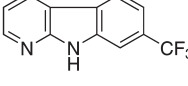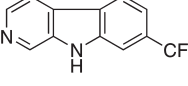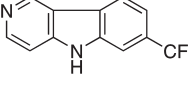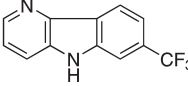
to the methylene group concomitantly with the formation of a carbazole core structure to provide the desired carbazole **12**.

The synthesis of compound **13a** with a urea group at the carbazole 2-position began from commercially available pinacolboronate ester **33** (Scheme 4). Compound **33** was converted to the 2-nitrobiphenyl derivative **34** by Suzuki—Miyaura coupling, which underwent reductive cyclization to afford Boc-protected aminocarbazole **35**. After deprotection, compound **36** was converted to the expected carbazole **13a** by using KOCN.[22] Compound **13b** with a urea group at the carbazole 3-position was prepared by the existing method.[12]

Structure—Activity Relationship Study of Carboline- and Carbazole-Based KSP Inhibitors. The resulting carbolines and carbazoles were evaluated for inhibition of KSP ATPase and cytotoxicity toward HeLa cells. Among carboline derivatives **9a—d** having a 7-trifluoromethyl group, no inhibitory effect was observed by the α-carboline derivative **9a**, whereas β- and γ-carbolines **9b,c** exerted enhanced KSP ATPase inhibitory activity compared with the corresponding carbazole derivative **3a** or biaryl-type derivative **4** [IC$_{50}$(**9b**) = 0.052 μM; IC$_{50}$(**9c**) = 0.095 μM] (Table 1). δ-Carboline **9d** exhibited similar inhibitory potency to the parent carbazole **3a**. A positive correlation between KSP ATPase inhibition and cytotoxicity toward HeLa cells was observed among carboline-based KSP inhibitors **9a—d**; for example, the cytotoxicity of β-carboline **9b** was the most potent (IC$_{50}$ = 0.81 μM). This investigation revealed that the restriction of the rotatable bond in biaryl-type compounds using fused indole scaffolds is a promising approach to design potent KSP inhibitors.
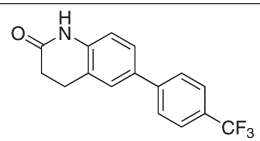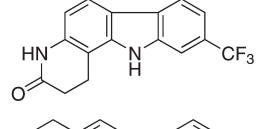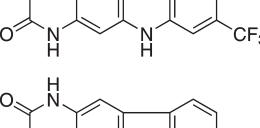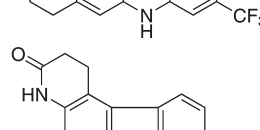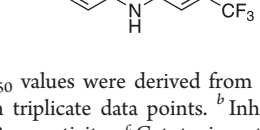
Carbazole derivatives **10a—d** with a lactam-fused structure were then investigated (Table 2). The accessory anilide group at the carbazole 2-position (**10a,b**) improved KSP ATPase inhibitory activity compared with **5**. Interestingly, carbazole **10b** with a 2,3-fused lactam ring showed remarkably potent cytotoxicity (IC$_{50}$ = 0.091 μM) in comparison with carbazole **10a** fused at the 1- and 2-positions, although **10b** showed approximately equipotent KSP ATPase inhibitory activity to **10a**.[23] An identical modification at the carbazole 3-position (**10c,d**) was less effective, which showed similar or slightly greater potency compared with the parent carbazole **3a**. This may be due to the inappropriate orientations of the lactam anilide moiety or the electron-donating effect to the carbazole scaffold. The 2,3-fused lactam **10c** did not show bioactivity in the cell-based assay, which was in contrast with **10b**, which had a similar fused ring systems.

Table 1. Structure—Activity Relationships of Carboline Derivatives

compound		KSP ATPase IC$_{50}$ (μM)[a, b]	cell growth IC$_{50}$ (μM)[a, c]
	3a	0.21	7.8
	4	> 6.3[d]	-[e]
	9a	> 6.3	> 200
	9b	0.052	0.81
	9c	0.095	1.4
	9d	0.33	16

[a] IC$_{50}$ values were derived from the dose—response curves generated from triplicate data points. [b] Inhibition of microtubule-activated KSP ATPase activity. [c] Cytotoxic activity against HeLa cells after 72-h exposure to each compound. [d] IC$_{50}$ was ∼10 μM. [e] Not tested.
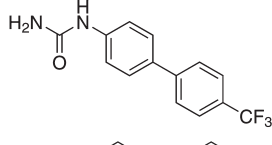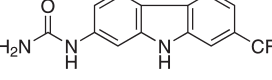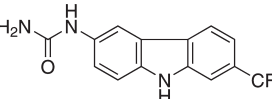
Table 2. Structure—Activity Relationships of Carbazole Derivatives with a Lactam-Fused Structure

compound		KSP ATPase IC$_{50}$ (μM)[a,b]	cell growth IC$_{50}$ (μM)[a,c]
	5	0.046	0.28
	10a	0.040	0.61
	10b	0.031	0.091
	10c	0.18	> 63
	10d	0.084	5.0

[a] IC$_{50}$ values were derived from the dose—response curves generated from triplicate data points. [b] Inhibition of microtubule-activated KSP ATPase activity. [c] Cytotoxic activity against HeLa cells after 72-h exposure to each compound.

Table 3. Structure−Activity Relationships of Carbazole Derivatives with a Urea Group

compound		KSP ATPase IC$_{50}$ (μM)^{a,b}	cell growth IC$_{50}$ (μM)^{a,c}
	6a	0.10	1.1
	6b	0.14	1.5
	13a	0.085	0.38
	13b	0.12	4.0

^{a} IC$_{50}$ values were derived from the dose−response curves generated from triplicate data points. ^{b} Inhibition of microtubule-activated KSP ATPase activity. ^{c} Cytotoxic activity against HeLa cells after 72-h exposure to each compound.
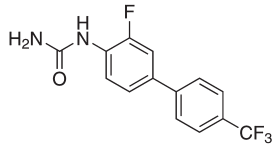
Table 4. Structure−Activity Relationships of Carbazole Derivatives with Five-, Six-, and Seven-Membered Lactam-Fused or Pyrrole-Fused Structures

compound		KSP ATPase IC$_{50}$ (μM)^{a,b}	cell growth IC$_{50}$ (μM)^{a,c}
	12	0.037	0.11
	10b	0.031	0.091
	11b	0.045	0.11
	11a	0.058	1.1
	31	0.17	2.7

^{a} IC$_{50}$ values were derived from the dose−response curves generated from triplicate data points. ^{b} Inhibition of microtubule-activated KSP ATPase activity. ^{c} Cytotoxic activity against HeLa cells after 72-h exposure to each compound.
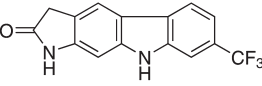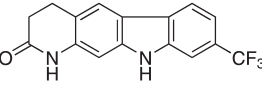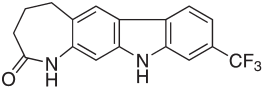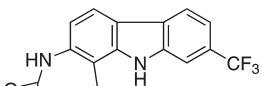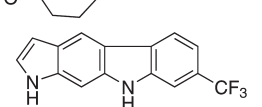
The outward orientation of the lactam NH group in 10c was disadvantageous to the interaction with KSP and cellular effects.

The biological activities of urea-containing compounds were also examined (Table 3).[12] The urea group at the carbazole 2-position in 13a slightly improved KSP ATPase inhibitory activity and cytotoxicity compared with the biphenyl-type inhibitors 6a,b. 3-Carbamidylcarbazole 13b was less potent than the 2-substituted congener 13a, which was consistent with the series of carbolines 9a−d and lactam-fused compounds 10a−d.

Subsequently, optimization of the lactam ring was carried out for the highly potent carbazoles 10a,b (Table 4). Carbazole derivatives 12 and 11b, which were fused at the carbazole 2,3-positions with a five- and seven-membered lactam, respectively, exerted slightly less bioactivity compared with the six-membered lactam 10b, suggesting the great flexibility of the lactam carbonyl placement. Inhibitory activity was also dependent upon the position of ring fusion. Carbazole 11a, which was fused with a seven-membered lactam at the 1- and 2-positions, showed less KSP inhibition and cytotoxicity than the 2,3-fused congener 11b. This was consistent with the bioactivity profiles of compounds 10a,b with a six-membered lactam. The less potent activities of pyrrolocarbazole derivative 31 than 12 indicate that a lactam carbonyl group at this position is an indispensable functional group for bioactivity.

Examinations of three series of carboline and carbazole derivatives revealed that the appropriate restriction of the rotatable linkage in biphenyl-type compounds provides favorable effects on KSP ATPase inhibitory activity and cytotoxicity. Introduction of a direct NH linkage in the original biphenyls 4−6 stabilized the coplanar conformation and bidirectional arrangements of two accessory groups to fabricate the potential interactions with the enzyme. Although twisted bioactive conformations of two phenyl rings in 5 for KSP were proposed,[10b] the potent constrained analogs 10a,b suggest that the planar conformations could provide another favorable interaction for bioactivity. In particular,

modification at the carbazole 2-position with a polar group such as a nitrogen atom (for β-carboline), lactam amide, or urea group improved the inhibitory activities. The lactam-fused carbazole 10b with a linear 6−6−5−6 fused ring system was the most potent KSP inhibitor in this investigation.

Potent KSP inhibitors (10a,b and 13a) were evaluated for inhibitory effects against the other motor proteins: centromere-associated protein E (CENP-E), Kid, mitotic kinesin-like protein 1 (MKLP-1), and KIF-4 (see Supporting Information). The compounds did not inhibit these kinesins even at 20 μM, indicating that they are specific KSP inhibitors. Furthermore, we investigated the effects of these compounds on cell cycle progression (Table 5). All of these compounds triggered cell-cycle arrest of HeLa cells to accumulate mitotic cells, and in particular, lactam-fused carbazole 10b was effective in a low MI$_{50}$ (50% mitotic index induction concentration). In the microscopic analysis of the mitotic phenotype of the cells treated with highly potent β-carboline 9b, carbazoles 10a,b, and 13a, the formation of monopolar spindles (the typical phenotype of KSP inhibition) was observed in all of the mitotically arrest cells (Figure 3 and the Supporting Information). Although β-carbolines were reported to inhibit topoisomerases I/II,[24] the possible off-target effects were not observed by treatment with 9b.

Mechanistic Studies of Carboline- and Carbazole-Based KSP Inhibitors. It has been reported that most KSP inhibitors (e.g., monastrol, S-trityl-L-cysteine) bind to the allosteric pocket formed by helices α2 and α3 and loop L5.[25,26] For example, tetrahydrocarboline-based inhibitors such as 2 (which was a lead compound for our carbazole-based inhibitors 3a−c) also bind to the same allosteric pocket to show ATP-uncompetitive behavior.[27] In contrast, the biphenyl-type inhibitors 5 and 6a (which work in an ATP-competitive manner) bind at the interface of helices α4 and α6 of the KSP ATPase domain (not at the ATP binding site).[10b]

Table 5. Effects of KSP Inhibitors on Cell Cycle Progression of HeLa Cells

compound	MI$_{50}$ (μM)[a]
5	0.29
6b	3.7
10a	1.1
10b	0.13
13a	1.3

[a] MI$_{50}$ values indicate the concentration of 50% induction in mitotic HeLa cells after 24-h exposure to each compound. Values were derived from dose—response curves generated from triplicate data points.
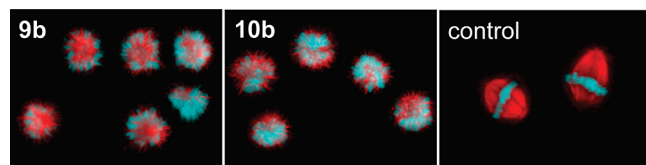
Figure 3. Mitotic phenotype of HeLa cells treated with fused indole derivatives **9b** (8.0 μM) and **10b** (0.25 μM). Chromosomes are colored blue and microtubules red.
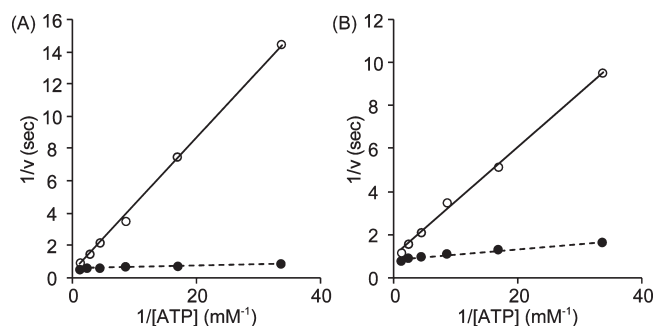
Figure 4. Lineweaver—Burk plots of the kinetics of KSP ATPase. ATPase activity of 80 nM KSP motor domain with 400 nM microtubules as a function of ATP concentration in the absence (●) and presence (○) of inhibitors were measured by steady-state KSP ATPase assay. (A) β-carboline **9b** (56 nM); (B) lactam-fused carbazole **10b** (32 nM). Each data point is the average of two independent experiments. Enzyme velocities at the same inhibitor concentration were fitted to the Michaelis—Menten equation to obtain V_{max}.

The carboline- and carbazole-based inhibitors **9**—**13** were designed by a combination of two distinct scaffolds (ring-fused compounds **1**—**3** and biaryl compounds **4**—**6**) so the inhibitory mechanism and binding site of KSP inhibitors **9**—**13** would be of interest.

To provide valuable insights into the binding mode of inhibitory β-carboline **9b** and lactam-fused carbazole **10b**, KSP ATPase activity was assessed in the absence or presence of inhibitors when incubated with variable ATP concentrations (Figure 4). Lineweaver—Burk plots revealed consistent V_{max} values independent of the presence of the inhibitors. This indicated that compounds **9b** and **10b** functionally compete with ATP binding.[28] It is of interest that these inhibitors **9b** and **10b** worked in a similar mode of inhibition to biphenyl-type **4**—**6** even though these belong to different types of scaffolds. This is the first observation of β-carboline and carbazole scaffolds for potent ATP-competitive KSP inhibitors.

Preliminary docking simulation study of these inhibitors demonstrated that the adenine binding pocket at the ATP binding site was too small to accommodate the potent lactam-fused carbazole **10b** (data not shown). In addition, reported crystal structure analyses[29] revealed that the structures of the ATP binding site were highly conserved between KSP and CENP-E. This suggested that possible binding of these inhibitors to the nucleotide site would be contradictory to high KSP selectivity. Accordingly, it is likely that these carboline and carbazole derivatives bind to the interface of helices α4 and α6 in a similar binding mode to biphenyl-type inhibitors.

■ CONCLUSIONS

We identified a novel class of small-molecule KSP inhibitors. Studies of the structure—activity relationship of carboline and carbazole derivatives indicated that the coplanar conformations of biphenyl groups favorably contribute to potent KSP inhibition. In addition, hydrophilic groups (e.g., lactam amide group) at the appropriate position are also indispensable functional groups. The carbazole derivative **10b** fused with a six-membered lactam at the 2- and 3-positions exhibited the most potent KSP ATPase inhibitory activity and the consequent cytotoxicity by effective cell-cycle arrest at the M-phase. It can be concluded from the biochemical studies and selectivity profiles for several kinesins that the carbolines and carbazoles work as ATP-competitive KSP inhibitors by presumably binding at the same site to the one for the parent biphenyl-type inhibitors. These investigations suggest that similar fused indole scaffolds may provide two distinctive KSP inhibitors, which work through separate inhibitory modes: tetrahydrocarboline-based ATP-uncompetitive inhibitors such as **2** and planar carboline/carbazole-based ATP-competitive inhibitors such as **9b** and **10b**.

■ EXPERIMENTAL SECTION

General. ^{1}H NMR spectra were recorded using a JEOL AL-400 or a JEOL ECA-500 spectrometer. Chemical shifts are reported in δ (ppm) relative to Me$_4$Si as an internal standard. ^{13}C NMR spectra were referenced to the residual CHCl$_3$ signal. Exact mass (HRMS) spectra were recorded on a JMS-HX/HX 110A mass spectrometer. Melting points were measured by a hot stage melting point apparatus (uncorrected). For flash chromatography, Wakogel C-300E (Wako) was employed. For analytical HPLC, a Cosmosil 5C18-ARII column (4.6 × 250 mm, Nacalai Tesque, Inc., Kyoto, Japan) was employed with a linear gradient of CH$_3$CN containing 0.1% (v/v) TFA at a flow rate of 1 mL/min on a Shimadzu LC-10ADvp (Shimadzu Corp., Ltd., Kyoto, Japan), and eluting products were detected by UV at 220 nm. The purity of the compounds was determined by combustion analysis or HPLC analysis (>95%).

KSP ATPase Assay. The microtubule-stimulated KSP ATPase reaction was performed in a reaction buffer [20 mM PIPES-K (pH 6.8), 25 mM KCl, 2 mM MgCl$_2$, 1 mM EGTA-KOH (pH 8.0)] containing 38 nM bacteria-expressed KSP motor domain (1—369) fused to a histidine tag at the carboxyl terminus and 350 nM microtubules in 96-well half-area plates (Corning). Each chemical compound in DMSO at different concentrations was diluted 12.5-fold with the chemical dilution buffer [10 mM Tris-OAc (pH7.4), 0.04% (v/v) NP-40]. After preincubation of 9.7 μL of the enzyme solution with 3.8 μL of each chemical solution at 25 °C for 30 min, the ATPase reaction was initiated by the addition of 1.5 μL of 0.3 mM ATP, followed by incubation at 25 °C for a further 15 min. The reaction was terminated by the addition of 15 μL of the Kinase-Glo Plus reagent (Promega). The ATP consumption in each

reaction was measured as the luciferase-derived luminescence by ARVO Light (PerkinElmer). At least three experiments were performed per condition, and the averages and standard deviations of inhibition rates in each condition were evaluated to determine IC_{50} values using Microsoft Excel and GraphPad Prism software.

Growth Inhibition Assay. HeLa cells were cultured in DMEM medium supplemented with 10% (v/v) FCS and antibiotics at 37 °C in a 5% CO_2 incubator. Growth inhibition assays using HeLa cells were performed in 96-well plates (Greiner). HeLa cells were seeded at 5000 cells/well in 50 μL of DMEM and placed for 6 h. Chemical compounds in DMSO were diluted 100-fold with the culture medium in advance. Following the addition of 40 μL of the fresh culture medium, 30 μL of the chemical diluents were also added to the cell cultures. The final volume of DMSO in the medium was equal to 0.25% (v/v). The cells under chemical treatment were incubated for a further 72 h. The wells in the plates were washed twice with the cultured medium without phenol red. After 1 h incubation with 100 μL of the medium, the cell culture in each well was supplemented with 20 μL of the MTS reagent (Promega), followed by incubation for an additional 40 min. Absorbance at 590 nm of each well was measured using a VersaMax plate reader (Molecular Devices). At least three experiments were performed per condition, and the averages and standard deviations of inhibition rates in each condition were evaluated to determine IC_{50} values using Microsoft Excel and GraphPad Prism software.

Evaluation of Mitotic Arrest. HeLa cells were seeded at 10^5 cells/well in 500 μL of the medium on Lab-Tek II 8-well CC2 glass chamber slides (Nalge Nunc). After 6-h incubation at 37 °C in a 5% CO_2 incubator, the culture medium was exchanged with 400 μL of fresh medium containing different inhibitors or DMSO, and the cells were placed at 37 °C in 5% CO_2 for 24 h. The final volume of inhibitor dissolved in DMSO in the medium was 0.4% (v/v). Before processing for immunofluorescence, HeLa cells were washed once with PBS(−) and then fixed with 3% paraformaldehyde/PBS(−) for 3 min and then with MeOH at −20 °C for 10 min. Microtubules were stained with a primary mouse monoclonal anti-α-tubulin antibody, DM1A, and a secondary rabbit polyclonal AlexaFluor594-conjugated anti-mouse antibody (Molecular Probes). Mitotic chromosomes were stained with a primary polyclonal rabbit anti-phospho-histone H3 (Ser10) antibody (Upstate) followed by a secondary polyclonal AlexaFluor488-conjugated anti-rabbit antibody. DNA was counterstained with DAPI. Cells were classified as "mitotic", "interphase", or "other" by visual inspection to calculate the percentage of mitotic cells at each inhibitor concentration. At least 500 cells were examined per condition, and MI_{50} values were evaluated using Microsoft Excel and GraphPad Prism software. Fluorescent images were taken by a DP30BW CCD camera coupled to an IX71 microscope (Olympus) and superimposed using Adobe Photoshop software.

Steady-State KSP ATPase Assay. An enzyme-coupled system that regenerates ADP to ATP was used to measure ATP hydrolysis by KSP, with NADH absorbance at 340 nm as an indirect measurement of ATP turnover. To measure KSP ATPase activity in a reaction, the assay buffer [2.5 mM KCl, 50 mM PIPES (pH 6.9), 1 mM $MgCl_2$, 3 mM potassium phophoenol pyruvate, 450 μM $Na_2 \cdot$NADH, 1 mM dithiothreitol, 8 μM taxol, 9 U/mL lactate dehydrogenase, 15 U/mL pyruvate kinase, and 400 nM taxol-stabilized microtubules, and 80 nM bacteria-expressed KSP motor domain; K_m(ATP) = 15−35 μM] was supplemented with various concentrations of ATP along with KSP inhibitor solution. The optical density of a reaction at 340 nm was measured every 5 s using a UV-2450 photometer (Shimadzu). The steady-state rate of absorbance reduction was calculated using a linear least-squares fitting method by Shimadzu UVProbe version 2.10 and Microsoft Excel. The coupling activity of the ATP regeneration enzyme system was 100-fold greater than the ATPase activity measured in these experiments. Enzyme velocities were fitted to the Michaelis−Menten equation as a function of

ATP concentration at a particular drug concentration: $V = ([ATP] \times V_{max})/([ATP] + K_m)$.

■ ASSOCIATED CONTENT

ⓢ Supporting Information. Experimental procedures, characterization, and bioassay data. This material is available free of charge via the Internet at http://pubs.acs.org.

■ AUTHOR INFORMATION

Corresponding Author
*Tel: +81-75-753-4551. Fax: +81-75-753-4570. E-mail: soishi@pharm.kyoto-u.ac.jp (S.O.); nfujii@pharm.kyoto-u.ac.jp (N.F.).

■ ACKNOWLEDGMENT

■ ABBREVIATIONS

CENP-E,centromere-associated protein E; KSP,kinesin spindle protein; MKLP-1,mitotic kinesin-like protein 1

■ REFERENCES

(1) (a) Dutcher, J. P.; Novik, Y.; O'Boyle, K.; Marcoullis, G.; Secco, C.; Wiernik, P. H. 20th-century advances in drug therapy in oncology - part II. *J. Clin. Pharmacol.* **2000**, *40*, 1079–1092. (b) Jordan, M. A.; Wilson, L. Microtubules as a target for anticancer drugs. *Nat. Rev. Cancer* **2004**, *4*, 253–265.

(2) (a) Rowinsky, E. K.; Chaudhry, V.; Cornblath, D. R.; Donehower, R. C. Neurotoxicity of taxol. *J. Natl. Cancer Inst. Monogr.* **1993**, *15*, 107–115. (b) Quasthoff, S.; Hartung, H. P. Chemotherapy-induced peripheral neuropathy. *J. Neurol.* **2002**, *249*, 9–17.

(3) Sawin, K. E.; LeGuellec, K.; Philippe, M.; Mitchison, T. J. Mitotic spindle organization by a plus-end-directed microtubule motor. *Nature* **1992**, *359*, 540–543.

(4) (a) Blangy, A.; Lane, H. A.; d'Herin, P.; Harper, M.; Kress, M.; Nigg, E. A. Phosphorylation by p34cdc2 regulates spindle association of human Eg5, a kinesin-related motor essential for bipolar spindle formation in vivo. *Cell* **1995**, *83*, 1159–1169. (b) Walczak, C. E.; Vernos, I.; Mitchison, T. J.; Karsenti, E.; Heald, R. A model for the proposed roles of different microtubule-based motor proteins in establishing spindle bipolarity. *Curr. Biol.* **1998**, *8*, 903–913. (c) Tao, W.; South, V. J.; Zhang, Y.; Davide, J. P.; Farrell, L.; Kohl, N. E.; Sepp-Lorenzino, L.; Lobell, R. B. Induction of apoptosis by an inhibitor of the mitotic kinesin KSP requires both activation of the spindle assembly checkpoint and mitotic slippage. *Cancer Cell.* **2005**, *8*, 49–59. (d) Marcus, A. I.; Peters, U.; Thomas, S. L.; Garrett, S.; Zelnak, A.; Kapoor, T. M.; Giannakakou, P. Mitotic kinesin inhibitors induce mitotic arrest and cell death in Taxol-resistant and -sensitive cancer cells. *J. Biol. Chem.* **2005**, *280*, 11569–11577.

(5) Sakowicz, R.; Finer, J. T.; Beraud, C.; Crompton, A.; Lewis, E.; Fritsch, A.; Lee, Y.; Mak, J.; Moody, R.; Turincio, R.; Chabala, J. C.; Gonzales, P.; Roth, S.; Weitman, S.; Wood, K. W. Antitumor activity of a kinesin inhibitor. *Cancer Res.* **2004**, *64*, 3276–3280.

(6) (a) Mayer, T. U.; Kapoor, T. M.; Haggarty, S. J.; King, R. W.; Schreiber, S. L.; Mitchison, T. J. Small molecule inhibitor of mitotic spindle bipolarity identified in a phenotype-based screen. *Science* **1999**, *286*, 971–974. (b) Sarli, V.; Giannis, A. Inhibitors of mitotic kinesins: next-generation antimitotics. *ChemMedChem* **2006**, *1*, 293–298. (c) Jackson, J. R.; Patrick, D. R.; Dar, M. M.; Huang, P. S. Targeted antimitotic therapies: Can we improve on tubulin agents? *Nat Rev. Cancer*

2007, 7, 107–117. (d) Matsuno, K.; Sawada, J.; Asai, A. Therapeutic potential of mitotic kinesin inhibitors in cancer. *Expert Opin. Ther. Pat.* **2008**, *18*, 253–274. (e) Sarli, V.; Giannis, A. Targeting the kinesin spindle protein: Basic principles and clinical implications. *Clin. Cancer Res.* **2008**, *14*, 7583–7587.

(7) Oishi, S.; Watanabe, T.; Sawada, J.; Asai, A.; Ohno, H.; Fujii, N. Kinesin spindle protein (KSP) inhibitors with 2,3-fused indole scaffolds. *J. Med. Chem.* **2010**, *53*, 5054–5058.

(8) Nakazawa, J.; Yajima, J.; Usui, T.; Ueki, M.; Takatsuki, A.; Imoto, M.; Toyoshima, Y.; Osada, H. A novel action of terpenedole E on the motor activity of mitotic Kinesin Eg5. *Chem. Biol.* **2003**, *10*, 131–137.

(9) Hotha, S.; Yarrow, J. C.; Yang, J. G.; Garrett, S.; Renduchintala, K. V.; Mayer, T. U.; Kapoor, T. M. HR22C16: A potent small-molecule probe for the dynamics of cell division. *Angew. Chem., Int. Ed.* **2003**, *42*, 2379–2382.

(10) (a) Parrish, C. A.; Adams, N. D.; Auger, K. R.; Burgess, J. L.; Carson, J. D.; Chaudhari, A. M.; Copeland, R. A.; Diamond, M. A.; Donatelli, C. A.; Duffy, K. J.; Faucette, L. F.; Finer, J. T.; Huffman, W. F.; Hugger, E. D.; Jackson, J. R.; Knight, S. D.; Luo, L.; Moore, M. L.; Newlander, K. A.; Ridgers, L. H.; Sakowicz, R.; Shaw, A. N.; Sung, C. M. M.; Sutton, D.; Wood, K. W.; Zhang, S. Y.; Zimmerman, M. N.; Dhanak, D. Novel ATP-competitive kinesin spindle protein inhibitors. *J. Med. Chem.* **2007**, *50*, 4939–4952. (b) Luo, L.; Parrish, C. A.; Nevins, N.; McNulty, D. E.; Chaudhari, A. M.; Carson, J. D.; Sudakin, V.; Shaw, A. N.; Lehr, R.; Zhao, H.; Sweitzer, S.; Lad, L.; Wood, K. W.; Sakowicz, R.; Annan, R. S.; Huang, P. S.; Jackson, J. R.; Dhanak, D.; Copeland, R. A.; Auger, K. R. ATP-competitive inhibitors of the mitotic kinesin KSP that function via an allosteric mechanism. *Nat. Chem. Biol.* **2007**, *33*, 722–726. (c) Rickert, K. W.; Schaber, M.; Torrent, M.; Neilson, L. A.; Tasber, E. S.; Garbaccio, R.; Coleman, P. J.; Harvey, D.; Zhang, Y.; Yang, Y.; Marshall, G.; Lee, L.; Walsh, E. S.; Hamilton, K.; Buser, C. A. Discovery and biochemical characterization of selective ATP competitive inhibitors of the human mitotic kinesin KSP. *Arch. Biochem. Biophys.* **2008**, *469*, 220–231. (d) Matsuno, K.; Sawada, J.; Sugimoto, M.; Ogo, N.; Asai, A. Bis(hetero)aryl derivatives as unique kinesin spindle protein inhibitors. *Bioorg. Med. Chem. Lett.* **2009**, *19*, 1058–1061.

(11) Asai, A.; Sawada, J.; Matsuno, K.; Ogo, N.; Nishigaki, J.; Kojima, M. Japanese Patent JP200923986, 2009.

(12) The urea-containing carbazoles appeared in the previous patent information; however, the biological data have not been reported: Dhanak, D.; Knight, S. D.; Moore, M. L.; Newlander, K. A. PCT Int. Appl. WO2006005063, 2006.

(13) Ackermann, L.; Althammer, A. Domino N-H/C-H bond activation: palladium-catalyzed synthesis of annulated heterocycles using dichloro(hetero)arenes. *Angew. Chem., Int. Ed.* **2007**, *46*, 1627–1629.

(14) Owens, A. P.; Nadin, A.; Talbot, A. C.; Clarke, E. E.; Harrison, T.; Lewis, H. D.; Reilly, M.; Wrigley, J. D. J.; Castro, J. L. High affinity, bioavailable 3-amino-1,4-benzodiazepine-based γ-secretase inhibitors. *Bioorg. Med. Chem. Lett.* **2003**, *13*, 4143–4145.

(15) (a) Ishiyama, T.; Murata, M.; Miyaura, N. Palladium(0)-catalyzed cross-coupling reaction of alkoxydiboron with haloarenes: A direct procedure for arylboronic esters. *J. Org. Chem.* **1995**, *60*, 7508–7510. (b) Ishiyama, T.; Miyaura, N. Chemistry of group 13 element–transition metal linkage: The platinum- and palladium-catalyzed reactions of (alkoxo)diborons. *J. Organomet. Chem.* **2000**, *611*, 392–402.

(16) Freeman, A. W.; Urvoy, M.; Criswell, M. E. Triphenylphosphine-mediated reductive cyclization of 2-nitrobiphenyls: A practical and convenient synthesis of carbazoles. *J. Org. Chem.* **2005**, *70*, 5014–5019.

(17) (a) Watanabe, T.; Ueda, S.; Inuki, S.; Oishi, S.; Fujii, N.; Ohno, H. One-pot synthesis of carbazoles by palladium-catalyzed N-arylation and oxidative coupling. *Chem. Commun.* **2007**, 4516–4518. (b) Watanabe, T.; Oishi, S.; Fujii, N.; Ohno, H. Palladium-catalyzed direct synthesis of carbazoles via one-pot N-arylation and oxidative biaryl coupling: Synthesis and mechanistic study. *J. Org. Chem.* **2009**, *74*, 4720–4726.

(18) Thompson, A. L. S.; Kabalka, G. W.; Akula, M. R.; Huffman, J. W. The conversion of phenols to the corresponding aryl halides under mild conditions. *Synthesis* **2005**, *4*, 547–550.

(19) (a) Azizian, H.; Eaborn, C.; Pidcock, A. Synthesis of organo-trialkylstannanes. The reaction between organic halides and hexaalkyldistannanes in the presence of palladium complexes. *J. Organomet. Chem.* **1981**, *215*, 49–58. (b) Furuya, T.; Strom, A. E.; Ritter, T. Silver-mediated fluorination of functionalized aryl stannanes. *J. Am. Chem. Soc.* **2009**, *131*, 1662–1663.

(20) Scott, W. J.; Crisp, G. T.; Stille, J. K. Palladium-catalyzed coupling of vinyl triflates with organostannanes. A short synthesis of Pleraplysillin-1. *J. Am. Chem. Soc.* **1984**, *106*, 4630–4632.

(21) Kumar, C. N. S. S. P.; Devi, C. L.; Rao, V. J.; Palaniappan, S. Use of pyridinium chlorochromate and reusable polyaniline salt catalyst combination for the oxidation of indoles. *Synlett* **2008**, *13*, 2023–2027.

(22) Wang, H.; Liu, L.; Wang, Y.; Peng, C.; Zhang, J.; Zhu, Q. An efficient synthesis of 4-alkyl-2(1H)-quinazolinones and 4-alkyl-2-chloroquinazolines from 1-(2-alkynylphenyl)ureas. *Tetrahedron Lett.* **2009**, *50*, 6841–6843.

(23) The varied cell membrane permeability could be attributable to the incompatible results between the in vitro KSP inhibition and cytotoxicity.

(24) Funayama, Y.; Nishio, K.; Wakabayashi, K.; Nagao, M.; Shimoi, K.; Ohira, T.; Hasegawa, S.; Saijo, N. Effects of β- and γ-carboline derivatives of DNA topoisomerase activities. *Mutat. Res.* **1996**, *349*, 183–191.

(25) Yan, Y.; Sardana, V.; Xu, B.; Homnick, C.; Halczenko, W.; Buser, C. A.; Schaber, M.; Hartman, G. D.; Huber, H. E.; Kuo, L. C. Inhibition of a mitotic motor protein: Where, how, and conformational consequences. *J. Mol. Biol.* **2004**, *335*, 547–554.

(26) (a) Kaan, H. Y. K.; Ulaganathan, V.; Hackney, D. D.; Kozielski, F. An allosteric transition trapped in an intermediate state of a new kinesin-inhibitor complex. *Biochem. J.* **2010**, *425*, 55–60. (b) Kim, E. D.; Buckley, R.; Learman, S.; Richard, J.; Parke, C.; Worthylake, D. K.; Wojcik, E. J.; Walker, R. A.; Kim, S. Allosteric drug discrimination is coupled to mechanochemical changes in the kinesin-5 motor core. *J. Biol. Chem.* **2010**, *285*, 18650–18661.

(27) Barsanti, P. A.; Ni, W. W. Z.; Duhl, D.; Brammeier, N.; Martin, E.; Bussiere, D.; Walter, A. O. The discovery of tetrahydro-β-carbolines as inhibitors of the kinesin Eg5. *Bioorg. Med. Chem. Lett.* **2010**, *20*, 157–160.

(28) Although the plots in the presence and absence of inhibitors converged, the possible mixed mode of inhibition by binding to the second site cannot be ruled out.

(29) Garcia-Saez, I.; Yen, T.; Wade, R. H.; Kozielski, F. Crystal structure of the motor domain of the human kinetochore protein CENP-E. *J. Mol. Biol.* **2004**, *340*, 1107–1116.